

Average Radiative Capture Cross Sections for 30- and 65-keV Neutrons

R. L. MACKLIN, J. H. GIBBONS, AND T. INADA*

Oak Ridge National Laboratory, Oak Ridge, Tennessee

(Received 2 November 1962)

Neutron radiative capture cross sections near 30 and 65 keV have been measured for a large number of elements by means of a large liquid scintillator and a pulsed neutron source. The results show definitive even vs odd A effects as well as systematic variations due primarily to effects of nuclear shells. Calculations of the scintillator efficiency for various capture γ -ray cascade modes are in good agreement with experimental results.

I. INTRODUCTION

A STUDY of the systematics of neutron capture cross sections in the keV range has been reported.¹ However, there were many elements not included in that survey mostly because samples had not been obtained. Samples were obtained for most of the remaining elements for $A < 210$. The total collection of results near 30 and 65 keV is presented in this paper in tabular form.

A major uncertainty in liquid scintillator tank measurements of radiative capture is the sensitivity of the efficiency of the tank to changes in, for example, the average γ -ray multiplicity. A series of calculations were made using a high-speed computer to obtain some quantitative information on these effects. The results, summarized in Appendix I, agree closely with the data.

II. EXPERIMENTAL TECHNIQUES

The ORNL 3-MV Van de Graaff was pre-acceleration pulsed at 8- μ sec intervals with pulse durations of 10 nsec and average proton currents of 1.5–2.0 μ A. Lithium and ZrT targets were used near threshold to provide 30- and 65-keV average neutron energy groups. The 8- μ sec pulsing interval decreased the scattered neutron background below that of the earlier experiments¹ where the pulse interval was 1.6 μ sec. With this reduction the environmental background became dominant.

The xylene-based liquid scintillator and associated electronics were as described in reference 1, using the arrangement of Fig. 1(a) therein. The beam pulse ("stop") signal was no longer derived from the target itself but from a capacitive pickup threaded by the proton beam at a more convenient location. This was done in order to obtain a better signal-to-noise ratio and wave form for the beam stop pulse. It also allowed more freedom in proton target geometry.

The samples measured 6 to 7 in. in diameter and up to $\frac{1}{2}$ in. in thickness. They were sealed in evacuated cans fabricated from 0.001-in. thick steel. In a few cases (Na, K, Ca) a fairly heavy (1 cm \times 2 cm) welded rim was also present as part of the container construction.

* Visiting scientist from National Institute of Radiological Sciences, Chiba, Japan.

¹ J. H. Gibbons, R. L. Macklin, P. D. Miller, and J. H. Neiler, Phys. Rev. 122, 182 (1961).

This rim contributed a fraction of a mb by absorption of neutrons first scattered by the sample, although it was out of the path of the direct neutron beam. Lead salts, oxides, and carbonates were used in a few cases where the elemental form was not suitable.

III. RESULTS

Cross sections were obtained for P, Cl, K, Ca, Ti, Mn, Ga, As, Se, Rb, Te, Ba, Eu, Hf, Re, Os, and Ir at 30 and 65 keV in the same manner as in reference 1. Indium was again adopted as a cross-section standard, assuming 763 mb at 30 keV and 448 mb at 65 keV. In addition Si, S, V, Co, Ge, Rh, Dy, and Er cross sections previously reported at only one of the energies were measured at the other energy.

The radiative capture cross section for element X is related to the net area under its time peak A_x and to a corresponding area for the standard element by

$$\sigma_x = \sigma_{std} \frac{A_x \nu_{std} f_{std}}{A_{std} \nu_x f_x}$$

\times (RSP correction) (APL correction),

where ν = atoms/cm², f = fraction of gamma-ray pulses

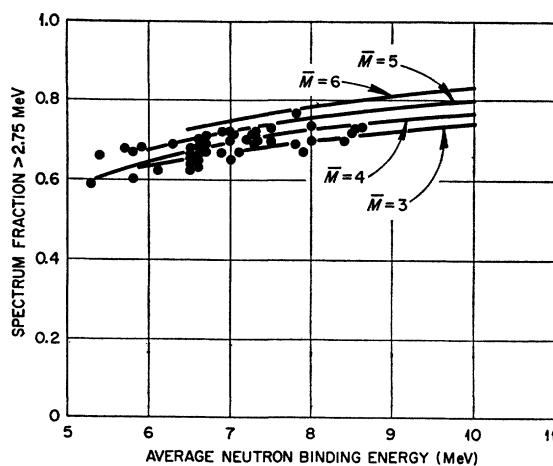


FIG. 1. Spectrum fraction vs average binding energy. The data points represent the fraction of capture pulses that produce a pulse height in the detector corresponding to or greater than 2.75 MeV. The solid lines are computed fractions for Maxwellian γ -ray cascades for several values of average multiplicity \bar{M} .

TABLE I. Results of "threshold" measurements with 30- and 65-keV average energy neutrons. Capture cross sections are given in mb. The estimated absolute error (standard deviation) as in the text is $\pm 9\%$ except where noted. The neutron energy resolution was approximately triangular with width at half-maximum of ± 7 and ± 20 keV at 30 and 65 keV, respectively.

Z	Element	$\sigma_{n,\gamma}(30)$	$\sigma_{n,\gamma}(65)$
6	C	<0.2	0.0 \pm 0.3
9	F	4.5 \pm 1.0	
11	Na	5.0 \pm 0.7	0.7 \pm 0.3
12	Mg	0.4 \pm 0.2	2.1 \pm 0.7
13	Al	2.8 \pm 0.7	
14	Si	13 \pm 4	2 \pm 0.7
15	P	7 \pm 1	0.5 \pm 0.2
16	S	25 \pm 8	0.8 \pm 0.6
17	Cl	11 \pm 4	4 \pm 2
19	K	16 \pm 2	4 \pm 1
20	Ca	10 \pm 1	3 \pm 1
22	Ti	29 \pm 3	5 \pm 1
23	V	23 \pm 8	3 \pm 1
24	Cr	10 \pm 3	3.5 \pm 1
25	Mn	22	9 \pm 1
26	Fe	12 \pm 3	6.3 \pm 2
27	Co	88 \pm 30	18
28	Ni	16 \pm 4	6.5 \pm 2
29	Cu	39 \pm 7	25 \pm 5
30	Zn	31 \pm 6	20 \pm 5
31	Ga	103	56
32	Ge	74	39 \pm 6
33	As	350	175
34	Se	94	51
35	Br	650	345
37	Rb	180	89
38	Sr	155	24
39	Y	13.5 \pm 3	6.9 \pm 2
40	Zr	14 \pm 3	10.3 \pm 2
41	Cb	264	135
42	Mo	140	69
45	Rh	850	540
46	Pd	454	265
47	Ag	951	586
48	Cd	330	183
49	In	(763)	(448)
50	Sn	88 \pm 15	51 \pm 10
51	Sb	436	245
52	Te	97	35
53	I	733	440
56	Ba	61	33
57	La	55 \pm 10	18 \pm 3
58	Ce	35 \pm 5	8 \pm 2
59	Pr	115	59
62	Sm	875	450
63	Eu	2560	1580
64	Gd	1175	670
65	Tb	1850	1070
66	Dy	775	570
67	Ho	1720	1070
68	Er	960	540
69	Tm	1310	700
70	Yb	575	390
71	Lu	2520	1200
72	Hf	510	330
73	Ta	735	440
74	W	270	190
75	Re	900	525
76	Os	300	175
77	Ir	795	450
78	Pt	330	234
79	Au	515	332
80	Hg	295	103
81	Tl	71	35
82	Pb	3 \pm 3	1 \pm 2
83	Bi	1 \pm 4	4 \pm 3
92	U ²³⁸	473	302

occurring within the detector single-channel analyzer window, RSP is resonance self protection and APL is average path length for neutrons in the sample material. The corrections were determined as indicated in reference 1. The determination of f , the spectrum fraction, was improved considerably by computer calculations of the pulse height distribution (see Appendix I). The combined data on f are shown in Fig. 1 plotted as a function of average binding energy. The solid curves are the calculated values for Maxwellian γ -ray cascades in very thin samples. The sample points refer to samples near 3 mm in thickness. Several sample thicknesses (up to 3 mm) of Ag, In, and Au were also measured experimentally. These tests showed that the spectrum degradation in the samples lowered the spectrum fraction about 0.04/mm of thickness from the very thin sample values. This coefficient undoubtedly also depends on binding energy, multiplicity, sample density and atomic number etc. to a minor extent.

The unusual spectrum shape observed in the rare earth region (Fig. 10, reference 1) has required the admixture of preferential dipole gamma decay via bound single-particle states as conjectured in reference 1. The relative importance of this effect peaks empirically near $A = 159$ with a width (full width at half-maximum) of about 15 amu. The natural width may be greater as the sensitivity of the pulse-height spectra falls off as the single-particle band energy departs from half the binding energy.

The combined results at 30 ± 7 and 65 ± 20 keV, including those from reference 1 are presented in Table I. The improved signal-to-background ratio has allowed us to set a closer limit (two standard deviations) on the 30 keV carbon cross section using the same sample. The new value is $\sigma < 0.2$ mb, replacing the value 0.2 ± 0.4 (one standard deviation) given in reference 1. The trend of the cross sections as a function of atomic number is indicated in Fig. 2 where the 65-keV data are shown graphically. The results for even and odd Z were plotted separately on semilog paper and then overlapped and normalized. The sharp dips corresponding to neutron shell closure for 50, 82, and 126 neutrons are clearly visible. The trend of the cross section in the region near the $Z = 50$ shell is complicated by the close proximity of $N = 82$ and the large number of isotopes of even nuclei.

The values of the even vs odd A target cross sections show a remarkably consistent difference of a factor of about 2.2, apparently independent of atomic weight. This same difference is noted for the 30-keV cross sections and may be associated with the "Bethe-Hurwitz effect" wherein the nuclear level spacing for even-even targets is "about a factor of two" over that of odd targets for $A > 45$.²

Errors are as noted in reference 1 except that the calculations of pulse shape have increased our confi-

² H. W. Newson and J. H. Gibbons, *Fast Neutron Physics* (Interscience Publishers, Inc., New York, 1962), Part II, Chap. V.L.

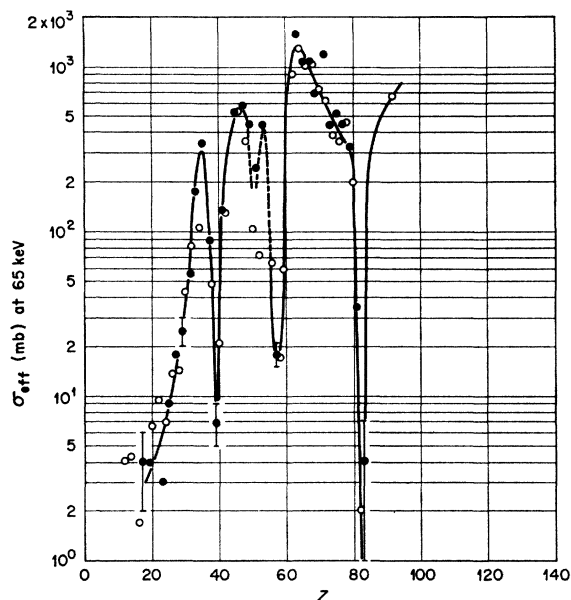


FIG. 2. Average radiative capture cross sections for 65-keV neutrons. The solid points correspond to results for odd- Z targets. The open circles correspond to results for even- Z targets where the even-even component result was empirically increased by a factor of 2.2 in order to cause the data to overlap. This even-odd effect is related to the average difference in level spacing for even vs odd nuclei. The effects of neutron shells at $N=50$, 82, and 126 are quite apparent. The proximity of the proton shell at $Z=50$ with $N=82$ may account for the large point scatter in the region $45 < Z < 55$.

dence in f . Accordingly, the error in the determination of the relative detector efficiency is considered reduced from 5 to 3%. The over-all minimum error estimate is thereby reduced from 10 to 9%, the major contributor (6%) is still the uncertainty in the cross-section standard.

APPENDIX I

The pulse-height response of the 1.2-m liquid scintillator for *single* gamma rays up to 10 MeV was computed

with the aid of a Monte Carlo code.³ The results were in good agreement with measurements on individual γ rays. The code was originally written for NaI(Tl) but, by replacing the cross sections could be adapted to other materials. The results from this calculation were fitted to smooth analytic formulas (that describe the response surface of pulse height vs E_γ vs relative counts) which were then built into a Monte Carlo cascade code.⁴ Cascades were constructed by (randomly) choosing gamma rays in succession from a Maxwellian energy distribution (of specified kT). The last gamma-ray energy chosen was reduced to make the total energy of each cascade equal the specified binding energy. The average multiplicity (number of gamma rays/cascade) was just one greater than the ratio of the binding energy to the value of kT . For each gamma ray, a pulse height was chosen at random from the distribution functions for single gamma rays and summed to give a pulse height for each cascade. The pulse-height distributions from this simple (Maxwellian) model fitted all our experimental data except the group near $A=159$ very well.

A further code was written to allow admixture of favored level transitions, for instance a Maxwellian cascade going to an excited state of the final nucleus or a two or three-step decay through specified levels competing (if desired) with the Maxwellian distribution. Finally, a Gaussian resolution broadening code allowed the results to be compared directly with the experimental data. The spectra near $A=159$ could only be fitted with a prominent admixture of a two-step transition to a band of levels about 1 MeV wide located at *half* the binding energy. This does not necessarily imply a very low multiplicity though ($\bar{M} < 3$, say), as low-energy transitions within the band or near the ground state would not have been distinguished.

³ C. D. Zerby and H. S. Moran, Nucl. Instr. Methods 14, 115 (1961).

⁴ Courtesy of N. Dismuke and others of the ORNL Mathematics Panel.